Int J Thermophys (2008) 29:2116–2125
DOI 10.1007/s10765-008-0541-7

Optothermoacoustic Phenomena in Highly Diluted Suspensions of Gold Nanoparticles

S. V. Egerev · A. A. Oraevsky

Published online: 20 November 2008

Abstract An optoacoustic (OA) sensor was designed, fabricated, and used to detect spherical gold nanoparticles (NPs) in diluted suspensions. The sensor, operating in the backward mode, was designed to measure signals from microscopic volumes of nanoparticulate suspensions in water. Thermal nonlinearity was observed in the course of OA signal generation. The irradiation of a microvolume of gold nanoparticles at the wavelength matching the peak of their plasmon resonance absorption gives rise to a multitude of thermomechanical processes, including heating of NPs below the critical temperature of water (374 K). The thermal diffusion from nanoparticles to water takes place; however, formation of vapor nanobubbles is avoided. As a result, a specific acoustic signal is produced exhibiting nonlinear behavior with respect to the incident laser pulse energy. The optoacoustic profile of the laser-induced signal generated in a thin layer of highly diluted suspensions of gold nanospheres was examined, thereby providing a basis for a method for detection of metal nanoparticles with high sensitivity.

Keywords Detection limits · Nanotechnology · Optoacoustic biosensor · Thermal nonlinearity

1 Introduction

The high sensitivity of optoacoustic systems has been utilized in absorption spectrophotometers and systems of laser ultrasonic testing and nondestructive defectoscopy.

S. V. Egerev (✉)
Andreyev Acoustics Institute, Moscow 117036, Russia
e-mail: sergey_egerev@mtu-net.ru

A. A. Oraevsky
Fairway Medical Technologies, 9431 W. Sam Houston Parkway South,
Houston, TX 77099, USA

Metal nanoparticles with strong plasmon resonance absorption, tunable in the visible and near-infrared spectral ranges, offer additional benefits for optoacoustic detection [1,2]. Laser interactions with suspensions of nanoparticles in aqueous media have been extensively studied in the past decade with the goal to develop biosensors and medical imaging and therapeutic applications [3]. Laser optoacoustics offers unique sensitivity for biosensors, cell and tissue imaging systems based on strongly absorbing metal (gold and silver) nanoparticles [4,5]. Theoretical and experimental studies into the physical mechanisms of sound generation in the course of thermal energy deposition in a medium by optical pulses are important for the development of optoacoustic methods for diagnostic and physicochemical analysis of such media [6,7]. An optoacoustic method combined with a statistical approach that helps to enhance detection sensitivity for metal nanoparticles in suspensions through detailed analysis of the spatial-temporal characteristics of an acoustic pressure response to pulsed laser impact has been suggested in our previous work and has shown promise; however, it required a statistically significant number of laser pulses [8]. In an effort to provide high-resolution OA detection, Frez et al. [9] used the transient grating method based on the formation of optical interference patterns from two-phase coherent laser beams.

This study had a goal to develop a sensitive optoacoustic method for detection of a small concentration and small volume of metal nanoparticles using a single laser pulse, or a small number of laser pulses. Thermodynamic processes in suspensions under exposure to the laser irradiation cause changes of the profile of the acoustic response as compared to that obtained from homogeneous solutions [3–8]. This phenomenon can be considered as an additional informative property for OA detection. Duration of the thermal relaxation in heterogeneous suspensions does not exceed 100 ns in a suspension containing particles with the largest dimension of 0.1 μm or less. Therefore, high temporal resolution is the most salient characteristic of this kind of OA detection method. In the past, several groups developed optoacoustic sensors with nanosecond resolution operating in the backward mode (front-surface transducers, FST) [10–14]. In the present paper we report results of studies of photothermoacoustic processes taking place in a thin layer of an ultra-diluted suspension of gold nanoparticles (NP) with the use of a wide-band FST sensor.

The idea of OA detection in heterogeneous disperse media containing absorbing nanoparticles is based on the significant contrast of optical and thermal parameters of particles and that of water. This means that absorption of optical energy occurs mainly in particles, but not in the surrounding medium (often water). The simplified approach to the stage-by-stage process of transformation of optical energy into the acoustic energy in water suspensions of NPs is presented by the five-stage scheme shown in Fig. 1.

When describing the first stage, it is necessary to know the dependence of an NP's optical absorption cross section on an NP's size, shape, and material. One of the most interesting properties of metal NPs is their extremely large cross section of optical absorption in the visible and near-infrared spectral range [2]. This increased optical absorption has a resonant character associated with excitation of so-called plasmon-polariton vibrations in the NPs. For spherical gold NPs, their optical properties can be described using the classical theory of Mie [15]. An approximate formula for an optical absorption cross section for spherical metal NPs is presented in [2,7]. For NPs

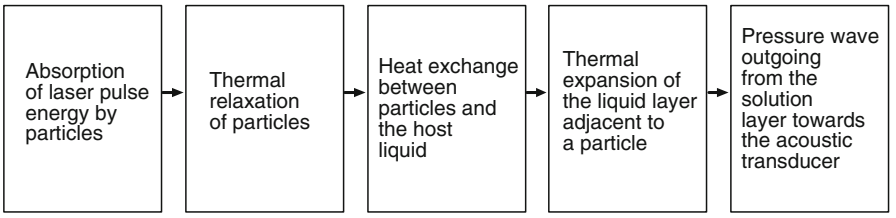

Fig. 1 Block diagram of physical processes upon optoacoustic detection of metal nanoparticles

having a diameter of $D = 200\,\text{nm}$ that were used in experiments, the absorption cross section σ at a wavelength of 532 nm is about two times greater than the physical cross section of the nanoparticle.

For the Q-switched laser used in our experiments with pulses of 12 ns in duration and nanoparticles with a diameter of 200 nm, we can calculate that the time of heat diffusion within the nanoparticles is much shorter than the laser pulse, $\tau_R \ll \tau_L$, where τ_L is the laser pulse duration. A simple estimate shows that the temperature equalization through the volume of a particle occurs on the time scale of picoseconds due to the high thermal conductivity of the nanoparticle material. The heat exchange between the NPs and the surrounding medium is generally determined by the ratio of their thermal conductivity coefficients $\psi_1/\psi_2 = \sqrt{(\kappa\rho C_p)_1/(\kappa\rho C_p)_2}$, where κ is the coefficient of thermal conductivity, ρ is the density, and C_p is the specific heat capacity. However, in the case of gold nanoparticles, $\psi_{NP} \gg \psi_{H2O}$, so that the heat is randomized instantly inside the NP, and the heat transfer to water is defined by the heat diffusion time $\tau_{HD} = R^2/6\chi$, where R is the nanoparticle radius and χ is the thermal diffusion coefficient of water [16]. The expression describing the increase of temperature of the nanoparticle during a laser pulse (i.e., when the particle simultaneously absorbs light and diffuses heat) can be presented in the following fashion [5]:

$$\Delta T_{NP} = \frac{F\sigma}{V_{NP}(\rho C_p)} \times \frac{\tau_{HD}}{\tau_L} \times \left[1 - \exp\left(-\frac{\tau_L}{\tau_{HD}}\right)\right], \tag{1}$$

where $F\,[\text{J}\cdot\text{m}^{-2}]$ is the incident laser fluence (upon the nanoparticle) and $\sigma = 6.2 \times 10^{-14}\,\text{m}^2$ is the plasmon-derived absorption by the 200 nm spherical gold nanoparticle at $\lambda = 532\,\text{nm}$, $V_{NP} = 4.19 \times 10^{-15}\,\text{ml}$ is the nanoparticle volume, $(\rho C_p)_{NP} = 2470\ \text{kJ}\cdot\text{m}^{-3}\cdot\text{K}^{-1}$ is the product of the density ($\rho = 19.3\ \text{g}\cdot\text{mL}^{-1}$) and specific heat capacity $C_p = 0.128\ \text{J}\cdot\text{g}^{-1}\cdot\text{K}^{-1}$ of gold, $\tau_{HD} = 0.5$ ns is the effective thermal diffusion time of the spherical gold nanoparticle, and $\tau_L = 10$ ns is the full temporal width of a Nd:YAG laser pulse assuming a top-hat profile.

Calculation of the temperature increase with the help of Eq. 1 yields $\Delta T_{NP} \cong 30\,\text{K}$ to 80 K. Thus, laser pulses create heat sources around gold nanoparticles with the temperature of water exponentially decreasing from the nanoparticle surface to the surrounding liquid. The thermal expansion of a superheated liquid leads to an effective generation of ultrasound in NP suspensions. As a result, the optoacoustic signal profile changes as compared to that from pure water (homogeneous weakly absorbing medium).

Intense heat exchange between the particles and the water can result in development of the so-called thermal nonlinearity when thermodynamic parameters of water in the course of this exchange do not remain constant. In particular, the coefficient of volumetric thermal expansion of water can experience a rapid increase. The coefficient of thermal nonlinearity for a homogeneous solvent can be expressed as

$$N = \frac{\partial\beta/\partial T}{\beta}\frac{\alpha\varepsilon}{\rho C_p} \approx 1, \tag{2}$$

where α and β are the optical absorption coefficient and the volumetric thermal expansion coefficient of water, respectively, and T stands for temperature.

In suspensions, the thermal nonlinearity will exhibit itself within the water layer immediately adjacent to the heated particle. Therefore, to describe thermal nonlinearity in suspensions, it would appear reasonable to introduce a new parameter of nonlinearity,

$$N_{\text{suspension}} = \frac{\partial\beta/\partial T}{\beta}\frac{3\sigma F}{4\pi\, R^3(\rho C_p)_{\text{NP}}}. \tag{3}$$

Evidently, for equal values of laser fluence, $N_{\text{suspension}} \gg N$. This inequality means that it is possible to choose a laser fluence value at which the thermal nonlinearity will result in a measurable increase of an optoacoustic signal in water suspensions of metal nanoparticles compared with that in pure water. This effect can be detected using a front-surface optoacoustic transducer (sensor). It can be found that the profile of a signal undergoes changes (amplitudes of the trailing edges of a signal noticeably increase). Also, a nonlinear dependence of amplitude of an acoustic signal as a function of laser fluence can be observed.

2 Front-Surface Optoacoustic Transducer

Two main experimental setups have been used for the OA detection of weakly absorbing liquids. The first, the so-called cylindrical scheme, employs an acoustic detector placed at a certain distance from the laser beam with its surface being parallel to the beam axis. This scheme lacks sensitivity in the range of high ultrasonic frequencies. In the alternative scheme used in our experiments, the laser beam is directed normal onto a thin sample layer, and acoustic detection is performed at the same site. In our experiments we dealt with the planar, layered configuration of excitation/detection. The laser beam was absorbed in the sample liquid layer confined between two optical elements made of quartz. To ensure planar geometry of the scheme, the parameters should meet the condition $2c_S\tau_L z/a^2 \ll 1$, where c_S is the sound speed in the medium separating a sample and a transducer (quartz), z is the distance from the sample to the transducer, and a is the laser beam diameter.

The acoustic transducer is parallel to the surface of the solution where the optoacoustic conversion takes place. These sensors are popular in studies of homogeneous solutions of low concentration. The unique advantages of this geometry have

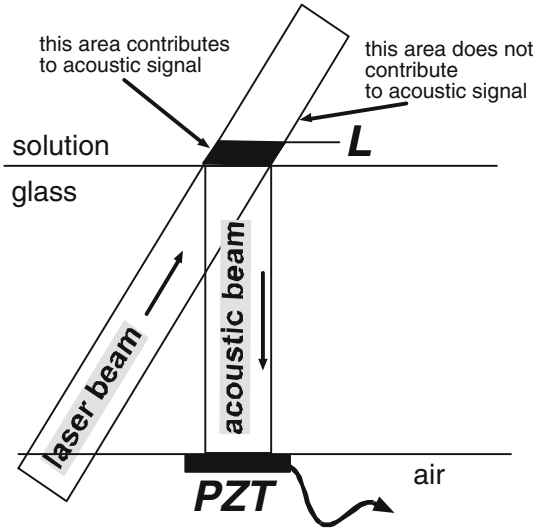

Fig. 2 General scheme of the front surface transducer (optoacoustic sensor)

been presented previously [17]. With the front surface transducer (FST) scheme, it is possible to measure the energetics and kinetics of processes occurring with lifetimes ranging from several nanoseconds to a few microseconds. Principles of formation of an acoustic signal in such a device are well known and are illustrated by a diagram of Fig. 2.

As follows from the scheme, the thickness of the volume of acoustic sources (i.e., the thickness of a layer of a NP suspension), which contribute to the overall optoacoustic signal, is very small and made approximately equal to the minimal detectable thickness. The detected thickness L of such an area, as presented in the optoacoustic signal, is equal to the greater of two sizes, $c_S \tau_L$ or c_S/f (where f is the detection system bandwidth). In our case, the latter was larger. For a detection band of 10 MHz, we have $L = 150\,\mu\text{m}$. Due to the necessity to generate one-dimensional geometry for propagating optoacoustic waves, we used a relatively wide laser beam with a diameter of 5×10^{-3} m.

The sensitivity of a FST is higher than that of conventional optoacoustic spectroscopy based on piezoelectric recording with a transducer positioned in the near-field of the acoustic sources. At a distance r from the acoustic source, the gain of sensitivity is equal to the ratio $G = \sqrt{a/r} \gg 1$ [10], where a is the laser beam diameter.

The front surface transducer (optoacoustic sensor) was implemented as a version of a layered prism cell (LPC). The LPC possesses enhanced temporal resolution and convenient experimental geometry of the FST [7]. The use of a cell made from a pair of prisms allows the laser beam to be transmitted through the sample and provides two surfaces parallel to the propagating planar acoustic wave to couple a piezoelectric transducer (see Fig. 3).

3 Experimental Setup

The NP suspensions and water samples were irradiated by an unfocused beam at a wavelength of the second harmonic (532 nm) radiation of a Nd:YAG laser with a pulse energy from 3×10^{-3} J to 0.2 J and a pulse length of 10 ns (see Fig. 3). Two experimental samples were used: distilled double-filtered water and an extra-diluted suspension of spherical gold NPs with a diameter of 200 nm. The probe was placed between the two prisms separated by a washer. The acoustic signal traveling through the lower prism reaches the PZT in 3.3 μs after the irradiation of a sample by the laser beam. The PZT represents a piezoceramic disc coupled to a thick (30 mm) ceramic substrate-dumper. The thickness of the PZT disc is 250 μm (which corresponds to the resonance frequency of 10 MHz), and the area of metallization is about 10^{-4}m^2. The capacity of the receiver is 6.8 nF, and the sensitivity is 30 μV · Pa^{-1}. The detected electronic signals were averaged over 100 acquisitions.

A peculiarity of this experiment was that we used a layered prism cell (LPC) with an adjustable sample layer thickness. Due to replaceable washer rings, the distance between the top and bottom prism was variable from 4×10^{-6} m up to 1.8×10^{-3}m.

Since we used a wide-band acoustic transducer sensitive within a passband of up to 10 MHz, the contribution to the overall signal at the maximal gap between prisms was due to two thin layers each having a thickness of 1.5×10^{-4}m adjacent correspondingly to the upper and lower prisms. As a result, we have two isolated wavelet signals, separated by a sufficient delay. The level of the second wavelet depends on the arrangement of the top prism with the amplitude repeatability being rather low. However, its presence allowed a performance test of the cell design as well as validation of the theoretical predictions.

It was evident, that for low-frequency pressure transducers acting within a frequency band of less than 1 MHz, it is necessary to use the LPC with the maximal gap between prisms. Using the PZT acting within the passband of up to 10 MHz (our case), it is possible to reduce the distance between prisms to 10^{-4} m or less. In our experiment, the sample thickness was maintained at a level of about 10^{-5} m.

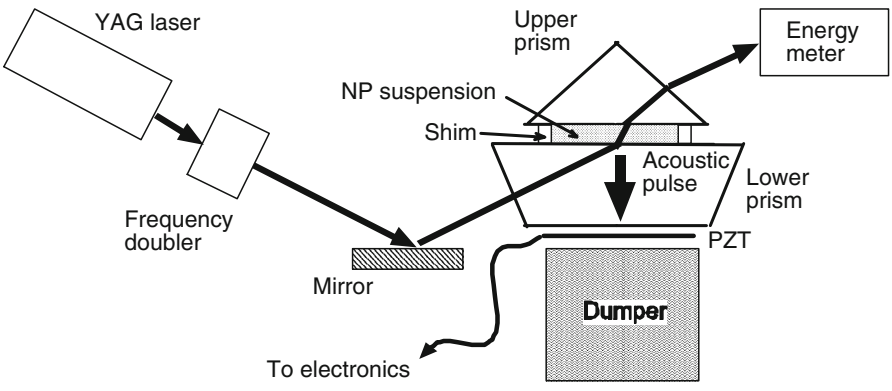

Fig. 3 Experimental setup of the optoacoustic experiment

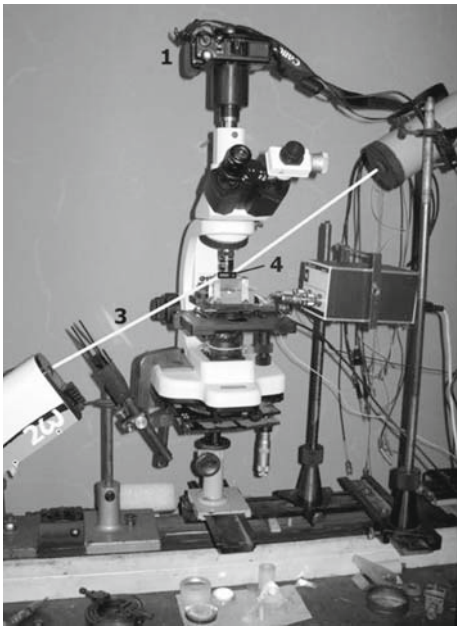

Fig. 4 A version of experimental setup. Additional equipment is a microscope (2) and digital camera (1) with the output fed to the PC. Here (3) is laser beam and (4) is the zone of optoacoustic conversion

To provide the real-time control of undesirable laser-induced cavitation phenomenon, the setup was modified with the help of a digital camera and a microscope (see Fig. 4). The dynamics of bubbles surrounding the overheated particle was observed at the PC monitor and the fluence was corrected correspondingly.

The suspension sample was prepared as follows. A volume of 0.08 ml of an NP suspension with a concentration $3.6 \times 10^{14} \mathrm{NP} \cdot \mathrm{m}^{-3}$ was diluted in 1.5 l of distilled water. The droplet of this suspension was positioned in the cell between the two prisms.

4 Results and Discussion

The results of time-resolved optoacoustic signal recording are presented in Figs. 5 and 6.

The laser irradiation of a pure water sample yields an acoustic signal represented with a solid curve, the irradiation of the NPs suspension yields an acoustic signal represented with a dotted curve. Laser fluence values varied from $320\,\mathrm{J} \cdot \mathrm{m}^{-2}$ and $480\,\mathrm{J} \cdot \mathrm{m}^{-2}$(Fig. 4) to $640\,\mathrm{J} \cdot \mathrm{m}^{-2}$and $800\,\mathrm{J} \cdot \mathrm{m}^{-2}$(Fig. 5). The left column shows raw signals after averaging over 64 laser pulses; the right column shows signals normalized to the maximum amplitude to reveal possible profile changes.

As can be seen from Fig. 4, the structure of an acoustic signal in a suspension differs from that in pure water. The analysis of the form of a signal shows a relative increase of a rarefaction phase of a signal from a suspension while the laser pulse fluence is increased to $800\,\mathrm{J} \cdot \mathrm{m}^{-2}$, which satisfies the theory of the thermal nonlinearity.

The magnitude of a signal exhibits nonlinear growth as a function of the laser fluence (Fig. 7). The nonlinear character of the dependence related to suspensions shows

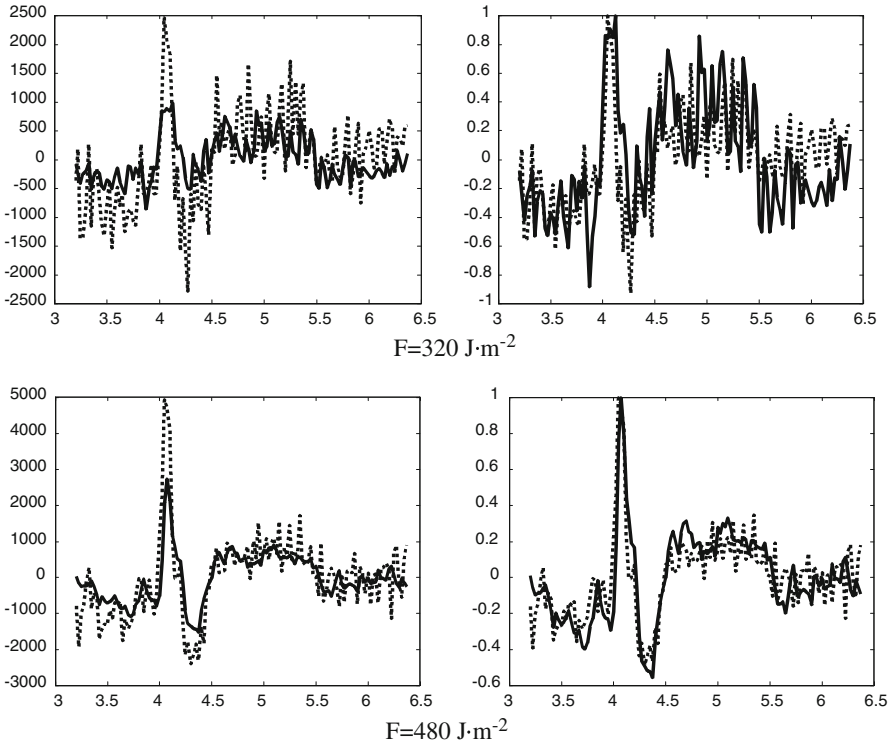

Fig. 5 Optoacoustic signal profiles experimentally measured in pure water (*solid line*) and strongly diluted suspensions of spherical gold nanoparticles (*dotted line*) at relatively low fluence irradiation: $320\,\mathrm{J}\cdot\mathrm{m}^{-2}$ (*upper set*) and $480\,\mathrm{J}\cdot\mathrm{m}^{-2}$ (*lower set*). Horizontal axis is in μs

the influence of thermal nonlinearity in suspensions. With a gradual increase of the laser fluence, the thermal nonlinearity can be better and better observed from the optoacoustic signal profile in water suspensions of gold nanoparticles. However, after the threshold fluence of about $1{,}000\,\mathrm{J}\cdot\mathrm{m}^{-2}$ is reached, the profiles of signals from both probes become indistinguishable and the informative value of the parameter of thermal nonlinearity is reduced. At laser fluence values greater than $1{,}000\,\mathrm{J}\cdot\mathrm{m}^{-2}$ laser irradiation provokes cavitation phenomena in the probe (see Fig. 8). This observation fits results of another study [18]. This effect and its informative opportunities for detecting NPs was investigated by our team previously [7].

5 Conclusion

We demonstrated that a small concentration of gold nanoparticles can be detected in water suspensions based on the thermal nonlinearity of optoacoustic signals. For each size (and corresponding optical absorption) of gold NPs, there is an optimal laser fluence that results in maximum difference between the optoacoustic signals in NP suspensions relative to the optoacoustic signals in pure water. Here we avoided

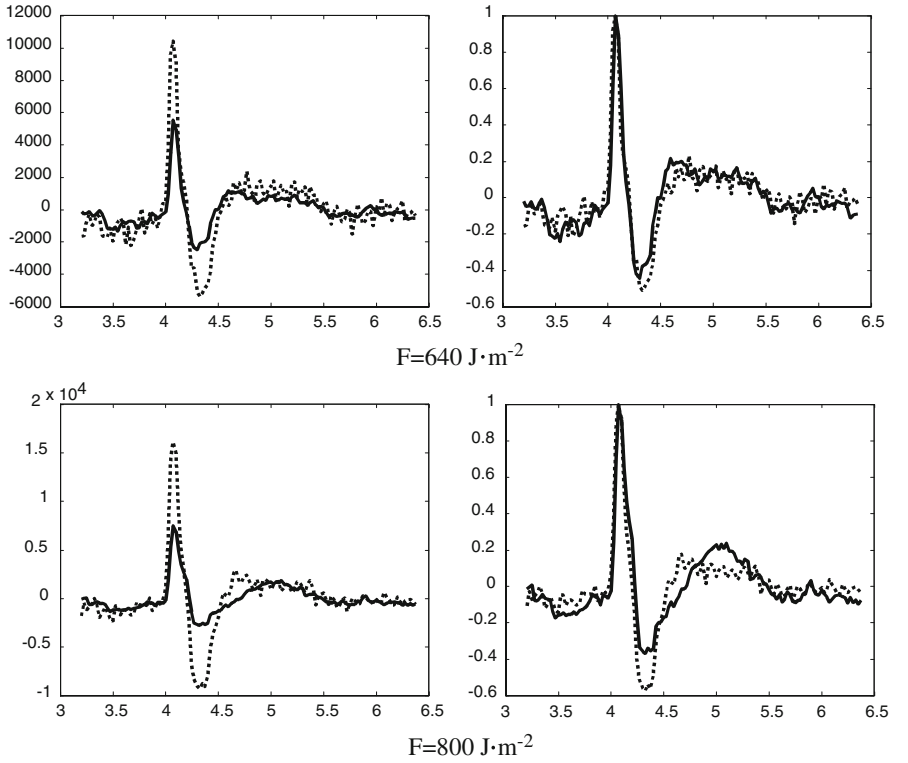

Fig. 6 Optoacoustic signal profiles experimentally measured in pure water (*solid line*) and strongly diluted suspensions of spherical gold nanoparticles (*dotted line*) at relatively high fluence irradiation: 640 J · m^{-2} (*upper set*) and 800 J · m^{-2} (*lower set*)

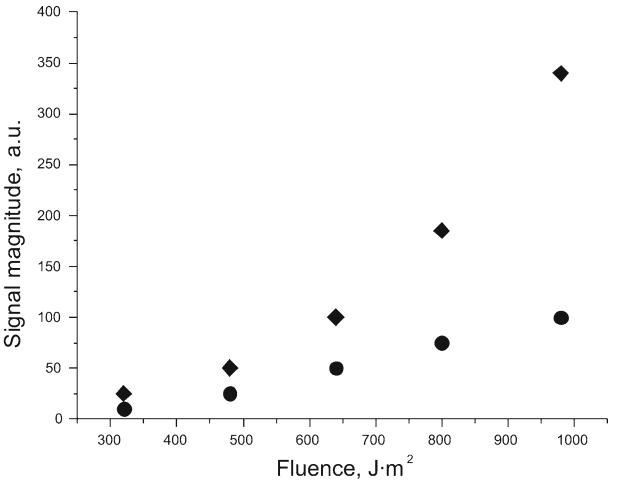

Fig. 7 Signal magnitude versus fluence for pure water (*circles*) and for suspension (*diamonds*)

Fig. 8 Photo through a microscope after a pulse having a fluence of about $1,000\,\mathrm{J}\cdot\mathrm{m}^{-2}$. The cavitation regime takes place at this fluence value. The maximum bubble diameter is $140\,\mu\mathrm{m}$

the superheating of NP by additional microscopic real-time control of the probable cavitation process.

Acknowledgments This work was supported in part by Grant # RP2-2494 from the US Civilian Research and Development Foundation, Grant # R44CA110137 from the National Cancer Institute, Grant # W81XWH-04-1-0484 from DoD/USAMRMC, and Grant # 07-02-00445-a from the Russian Foundation for Basic Research.

References

1. S.J. Oldenburg, R.D. Averitt, S.L. Wescott, N.J. Halas, Chem. Phys. Lett. **288**, 243 (1998)
2. D.V. Guzatov, A.A. Oraevsky, A.N. Oraevsky, Quantum Electron. **33**, 817 (2003)
3. N.G. Portney, M. Ozkan, Anal. Bioanal. Chem. **384**, 620 (2006)
4. A.A. Oraevsky, A.A. Karabutov, E.V. Savateeva, Proc. SPIE **4434**, 60 (2001)
5. J.A. Copland, M. Eghtedari, V.L. Popov, N. Kotov, N. Mamedova, M. Motamedi, A.A. Oraevsky, Mol. Imaging Biol. **6**, 341 (2004)
6. G. Diebold, M.I. Khan, S.M. Park, Science **250**, 101 (1990)
7. S. Ermilov, D.V. Huzatau, V.V. Klimov, A.P. Kanavin, A.A. Oraevsky, J. Appl. Phys. **99**, 123177 (2006)
8. S.V. Egerev, O.V. Ovchinnikov, A.V. Fokin, V.V. Klimov, D. Huzatau, A.P. Kanavin, A.A. Oraevsky, Proc. SPIE **5697**,73 (2005)
9. C. Frez, I.G. Calasso, G.J. Diebold, J. Chem. Phys. **124**, 034905 (2006)
10. S.V. Egerev, O.V. Puchenkov, Sov. Phys. Acoust. **31**, 30 (1986)
11. L. Melton, T. Hu, Q. Lu, Rev. Sci. Instrum. **60**, 3217 (1989)
12. A.A. Oraevsky, S.L. Jacques, R.O. Esenaliev, F.K. Tittel, Proc. SPIE **2134A**,122 (1994)
13. O. Puchenkov, S. Malkin, Rev. Sci. Instrum. **67**, 672 (1996)
14. T. Autrey, N.S. Foster, K. Klepzig, J.E. Amonette, J.L. Daschbach, Rev. Sci. Instrum. **69**, 2246 (1998)
15. G. Mie, Ann. Phys. (Paris) **25**, 377 (1908)
16. A.L. McKenzie, Phys. Med. Biol. **35**, 1175 (1990)
17. A.A. Karabutov, E.V. Savateeva, N.B. Podymova, A.A. Oraevsky, J. Appl. Phys. **87**, 2003 (2000)
18. A. Takami, H. Kurita, S. Koda, J. Phys. Chem. B **103**, 1226 (1999)